Platform-to-platform sample transfer, distribution, dilution, and dosing via electrothermal vaporization and electrostatic deposition[+])

G. Hermann[a,*], A. Trenin[a,b], R. Matz[a], M. Gafurov[a,b],

A.Kh. Gilmutdinov[b], K.Yu. Nagulin[b],

W. Frech[c], E. Björn[c], I. Grinshtein[d], L. Vasilieva[d]

[a]I. Physikalisches Institut, Justus-Liebig-Universität Giessen,

Heinrich-Buff-Ring 16, D-35392 Giessen, Germany

[b]Kazan State University, Kremlevskaja Str. 18, 420008 Kazan, Russia

[c]Department of Chemistry, University of Umea, SE-901 87 Umea, Sweden

[d]Russian Research Center "Applied Chemistry", Dobrolubova ave. 14, 197198

St. Petersburg, Russia

[+]) Dedicated to Prof. Dr. Drs. h.c. mult. Arthur Scharmann on the occasion of his 75th birthday.

* Corresponding author. Tel.: +49 641 99 33120; Fax: +49 641 99 33129;
e-mail: gerd.hermann@exp1.physik.uni-giessen.de

Abstract

A novel system for solid sample pretreatment, handling, and dosing for analytical atomic spectrometry is described. A primary solid or liquid sample is vaporized in a graphite furnace and then condensed in a specially designed condensation zone. On the further transport path, the analyte aerosol can be diluted and distributed in pre-set ratios in the laboratory made flow control system. Applying a corona discharge, aerosol particulates are then quantitatively re-collected by means of intra-furnace electrostatic precipitation on the platform of another graphite furnace or by external precipitation on one or a set of platforms. This makes possible to produce a set of secondary platforms with equal analyte compositions from one individual primary sample. Such multitudes allow sequential multi-element determinations with single-element instrumentation or comparative measurements with different techniques. Furthermore, the described procedure allows external thermal sample pretreatment with preceding pyrolysis and additional vaporization, condensation, and re-precipitation that significantly reduces or removes the sample matrix. Owing to different losses, transport efficiencies of electrothermal vaporization (ETV) instrumentation depend on analyte element, matrix, vaporization temperature, ramp rate, and tube history. In order to reduce the losses and therewith such dependencies of the losses, new laboratory constructed ETV unit with analyte condensation in an axially focusing upstream convection zone has been constructed. Analytical performance of the new setup is compared with the performance of a commercial end-on flow-through ETV unit when analyzing both liquid dosed samples and certified solid reference materials. The new system shows much higher transport efficiencies that are, in addition, more uniform for elements of different volatility. The effects of chemical sample modifiers and elements

supporting analyte condensation are studied. Most of the analytical measurements were carried out with a continuum source coherent forward scattering multi-element spectrometer. Comparative measurements were also carried out independently in the co-authors' laboratories with atomic absorption and inductively coupled plasma mass spectrometry techniques.

Keywords: Solid sampling; Electrothermal vaporization; Electrostatic precipitation; Transport efficiencies; Simultaneous multi-element determinations.

1. Introduction

Quantitative determination of trace elements in different matrices has become increasingly important in practically all areas of human activity. Electrothermal atomic absorption spectrometry (ET AAS) and inductively coupled plasma optical emission and mass spectrometry (ICP-OES and ICP-MS) are the most established techniques for the sensitive analysis of element trace concentrations. However, sample wet digestion with the risk of contamination and analyte losses, the use of concentrated acids at the sample preparation, and complications with analyte-matrix separation at the thermal sample pretreatment can considerably confine their application. These problems can be avoided by using direct solid sampling techniques [1].

Electrothermal vaporization (ETV) is one of the established means of sample introduction into ICP-OES/MS [1-11]. Less known is the use of an ETV as a solid sample pretreatment tool. In this case, a major part of the sample matrix is first removed by pyrolysis, then the analyte is vaporized in a furnace and carried away by an argon flow where its condensation occurs while being cooled. The analyte containing aerosol particulates can then be quantitatively re-collected by means of intra-furnace electrostatic precipitation (EP) on the wall of a graphite tube [12], or by external EP on a secondary graphite boat [13-15] or onto one or a set of secondary platforms by means of corona discharge applied to the deposition site [16-18].

In comparison with other techniques, the ETV-EP sampling offers some essential advantages. Samples can be introduced into the ETV unit directly as solids or liquids by means of the boat technique. Homogeneity of generated aerosols makes possible splitting and diluting the sample on the transport path in calibrated ratios. It allows the dosed

sample amount to be adapted to the dynamic range of an analytical instrument. Thus, primary solid sample can be weighed into the ETV boat in higher amounts in order to reduce dosing errors and effects caused by sample non-homogeneity, and thereby, to obtain higher precision and accuracy. The ETV-EP procedure includes external thermal sample pretreatment and a complete preceding distillation cycle (with vaporization, condensation, and re-precipitation) that allows significant sample matrix reduction [14]. The use of various chemical modifiers [19-21] allows further reduction of matrix effects and, moreover, facilitates the increase of the analyte transport efficiencies. It is suggested that foreign materials like added modifiers, matrix components, and gaseous phase additives [5, 10, 11, 22] improve co-vaporization and provide additional nucleation sites that speed up aerosol condensation [23] and, consequently, enhance the efficiency of analyte transport.

Commercially available or specifically designed graphite furnaces with vapor outlet through one of the ends of the graphite tube, end-on flow-through ETV (ETV-FT), were initially used as vaporization devices [4, 6-8, 10, 13, 14]. Detailed description of the time order of such ETV constructions was given by Lamoureux et al. [3]. Analytical performance of an ETV instrumentation can first of all be quantitatively characterized by analyte transport efficiency (TE) defined as the percentage ratio of analyte amount delivered to the spectrometer to the amount initially dosed into the ETV. Schäffer and Krivan [7] have indirectly measured TEs for eight elements of different volatility with an ETV-FT ICP-OES instrumentation using a radiotracer technique. As follows from this study, the major loss of elements occurs because of their retention on the colder outlet end of the graphite vaporizer. To decrease analyte deposition and thus improve TE, the authors

constructed a flow-through system with bypass gas entrance at the tube end [7]. With this improvement, they reported values ranging from 26-37% for elements of medium and low volatility to 35-57% for volatile elements. Another version of a flow-through ETV was suggested by Hassler and co-workers [10]. In their design, an internal nozzle as a part of the graphite tube was used. However, the most efficient way to prevent analyte deposition on the furnace colder ends turned out to be the ETV upstream configuration with the gas entering the furnace through its ends and flowing upwards through the hole in the graphite tube center. Such configurations were first presented by Kántor and Záray [2] for an indirect coupling to an ICP torch and by Lamoureux et al. [3] for simultaneous measurement of the atomic absorption and mass spectrometric signals. Later, Kántor and Güçer [9] determined the TE of five elements in the upstream ETV. They reported 67-76% for elements of medium volatility (Cu, Mn, Mg) and 32-38% for volatile elements (Cd, Zn). With addition of a carrier supporting gaseous modifiers these TEs could be increased to 67-73%. The masses of the analytes applied were 4-10 µg for each analyte. Based on comparative measurements, Kántor [11] has shown that the upstream ETV device is superior to that with vapor outlet through one of the tube ends.

In our laboratory [13-15], the TEs of 19-21% for medium volatile elements (Cu, Fe, Mn) and 36% for a volatile element (Pb) were obtained for organic certified reference materials vaporized in a commercially available ETV-FT unit (Grün AMS GmbH). Similar results were documented also for multi-element standard solutions containing approximately the same metal ratios as certified for the solid samples. Further measurements showed that the losses do not depend on the analyte element, only, but also on the matrix, the vaporization temperature, heating rate, and the tube age. Again, detailed investigations

have confirmed that the major losses of analytes occur due to their deposition onto the colder parts of the graphite tube, connecting tubing [6, 8], and under certain conditions within the ETV switching valve [8].

The potential of an ETV as a sample pretreatment and introduction tool arises from the fact that analyte aerosols generated in the furnace can then be quantitatively re-collected on other graphite platforms [17]. Consecutive elaboration of this idea resulted in the development of "Platform-to-Platform Sample Transfer, Distribution, Dilution, and Dosing System (PLASATRADIS)" that is presented in this paper. The system consists of the following three parts: 1) a modified electrothermal vaporizer, 2) aerosol transport control system that allows controllable flow ratios to be used for pre-designed analyte transportation, and 3) precipitation system consisting of one or ten equalized electrostatic precipitators. Integration of these parts into one unit provides a better way of coping with the problems associated with solid sample treatment. Furthermore, the quantitative platform-to-platform transfer allows direct determination of analyte TEs, since the primary and secondary samples can be obtained on the same types of boats that can be analyzed with the same analytical instrumentation.

The survey given above shows that the ETV instrument is the poorest part of the solid sample handling system. Based on the latest investigations, a new version of the ETV for the PLASATRADIS handling system is described in this paper. A main feature of this construction is the use of upstream configuration with the flow directed into a specially designed vertical tube that creates an axially focusing convection (AFC) zone, where particle condensation takes place away from the colder walls. The use of the upstream configuration allows significant reduction of analyte losses within the furnace while the use

of the AFC tube reduces their loss during further transportation. The aim is that with reducing the absolute analyte losses, their differences become reduced as well. The effects of added chemical modifiers and elements that increase analyte TE are also investigated in this work.

2. Experimental

2.1. Instrumentation

The ETV-AFC-EP arrangement is shown schematically in Fig. 1. The laboratory made electrothermal vaporizer consists of longitudinally heated pyrolytically coated graphite furnace (length, outer, and inner diameter are 53, 10, and 8 mm, respectively) with a 3 mm diameter transverse hole in the tube center that is used as the vapor outlet. The cross-cut of the vaporizer is given in Fig. 2a. The boat introduction is done by a pair of tweezers (see Fig. 2b) mounted on a sledge for reproducible transfer of the boat as a sample vessel into and out of the furnace, similar to that used in combination with the graphite furnace (SM30, GRÜN Analytische Mess-Systeme GmbH) for solid sampling atomic absorption spectrometry (SSAAS).

The ETV furnace has three gas inlets, one on each side of the graphite tube and one on the bottom of the unit. Both sides of the furnace are equipped with screwable windows to seal the furnace during the vaporization step. Tygon tubing (Norton, Akron, OH, USA) with 4 mm inner diameter connects the outlet of the ETV furnace with a glass capillary mounted on a laboratory constructed dosing arm of the AS-60 autosampler (Bodenseewerk Perkin-Elmer GmbH, Überlingen, Germany). For internal precipitation of

the analyte aerosol, the autosampler reproducibly inserts the glass capillary into the electrothermal atomization (ETA) furnace of the spectrometer through the sampling hole. A 100 µm tungsten wire with a sharp tip is placed in the glass capillary with a Y-formed end piece that combines the electrical and gas flow connections. The glass capillary is located approximately 2 mm above L´vov platform and directed against it. The platform is grounded while negative voltage of about 1.5 kV is applied via pre-resistors to the tungsten wire during the EP process in order to obtain a corona-like discharge. Further details of the electrostatic precipitator can be found elsewhere [12, 13, 16, 18].

Calibration of the ETV furnace at high temperatures was performed with optical pyrometer PB06F2 (Keller GmbH, Ibbenbueren, Germany). The drying and pyrolysis temperatures were measured with digital thermometer based on the thermocouple GTH 1200 A (Greisinger Electronic GmbH, Regenstauf, Germany). Table 1a shows the operating conditions of the ETV used in this work.

A laboratory-designed, computer-controlled continuum source coherent forward scattering spectrometer (ETA-CS-CFS, shortly CFS) is used for simultaneous multi-element analysis of the deposited particulates. The spectrometer is equipped with a continuum primary source (Xe short-arc lamp, XBO 450 W/4, Osram GmbH, Germany), a longitudinally heated ETA graphite furnace (HGA-600 with autosampler AS-60, Bodenseewerk, Perkin-Elmer GmbH, Überlingen, Germany), and an optical multi-channel analyzer (OMA, Model 1420 UV, EG&G, Princeton Applied Research, USA). The detector is coupled to a 0.25 m spectrograph (82-499, Jarell-Ash Europe S.A.). This arrangement allowed the simultaneous detection of line intensities within about 50 nm

wavelength interval. Further details of the spectrometer are given elsewhere [24-27]. Table 1b shows the operating conditions applied to the HGA-600 furnace.

Homogeneity of the analyte aerosol allows splitting and dilution of the sample on the transport path. The principles of aerosol transport, splitting, dilution, and dosing are schematically shown in Figs. 3a-c. Reduction of the analyte amount transported to the precipitator to a pre-set fraction 1/N after N-fold dilution of the sample aerosol is achieved in a specially designed aerosol flow splitting system shown in Fig. 3b. In this way the aerosol flow is split in a calibrated ratio

$$1 : (N - 1) \qquad (1)$$

i.e. into two sub-flows or into ten equal sub-flows (N = 10) when the highly-symmetric ten-fold splitter is employed (Fig. 3c). Thus, the pre-diluted sample amount that fits the dynamic range of an analytical instrument can be used for subsequent measurements. With using the ten-fold splitter, the ten aerosol sub-flows are subsequently precipitated onto ten different boats in the external ten-fold precipitator (Fig. 4a) yielding equal analyte compositions on the boats. Photos of the splitter, the precipitator, and secondary platform adapters for instruments of Analytik Jena AG, PerkinElmer, Gruen AMS GmbH, and others are shown in Figs. 4b-e, respectively.

2.2. Reference materials and reagents

The certified reference material BCR 189 Wholemeal flour (Institute of Reference Materials and Measurements, Geel, Belgium) is used to measure analyte TEs. The analyte concentrations used are listed in Table 2a. Multi-element standard solutions containing approximately the same element ratios as in the CRM are prepared by respective dilution of 1000 mg l^{-1} stock solutions of metal nitrates (Merck KGaA, Darmstadt, Germany) with

double distilled water to obtain a final concentration. To investigate modifier effects on analyte TEs, multi-element standard solutions are also prepared by diluting stock solutions (1000 mg l^{-1}) of Cu, Fe, Mn, Ni, Al, and Pb as nitrates. Corresponding analyte contents are listed in Table 2b. As sample/carrier modifier 1 µg K (as nitrate prepared from a standard stock solution) or 1 µg Pd (as diluted $Pd(NO_3)_2$ modifier solution) is added. Nitric acid of suprapur® grade (Merck KGaA, Darmstadt, Germany) is used. Argon of 99.996% purity (Messer Griesheim GmbH, Krefeld, Germany) is employed as internal and coolant gas.

2.3. Procedures

The solid sample (30-500 µg BCR CRM 189) is loaded onto the graphite boat and weighed on a balance (Model M5SA, Mettler, Zürich, Switzerland). After adequate pre-dilution, the appropriate volumes of multi-element standard solutions are injected manually onto the boat with a pipette (Eppendorf-Netheler-Hinz GmbH, Hamburg, Germany). Then, the boat is introduced into the ETV furnace. During the drying and pyrolysis steps the furnace is kept open and flushed with 1.5 L min^{-1} total Ar flow (Table 3). Gas enters from the rear end of the furnace, flows through the graphite tube and removes drying and pyrolysis products through the open fore end. This avoids contamination of the tubing and sampling capillary. Optimal pyrolysis and complete vaporization of the solid samples without visible matrix residues were obtained when adding 20 µl 5% nitric acid to the solid sample on the graphite boat and applying 350°C pyrolysis temperature [15]. After pyrolysis, the ETV furnace is closed and the gas flows are tuned to the final rates.

The high voltage is applied to the precipitator after 5 s delay. The vaporization step starts 10 s later. During the subsequent cool down step (stepwise during 60 s in order to

prevent reverse flow owing to gas contraction), the EP process is completed. Before starting the optional cleaning step, the high voltage is switched off and the autosampler removes the precipitation capillary from the atomizer. After dosing the sample into the ETV the whole measurement cycle takes about 4-5 min.

The analyte TEs are determined by comparing the results obtained by dosing the multi-element standard solution directly into the HGA furnace of the CFS spectrometer with those obtained by the full ETV-EP CFS procedure. Peak areas are used as analytical signals for calibration.

To obtain ten secondary samples with equal analyte compositions, a primary platform with twentyfold amount of analytes is introduced into the ETV and vaporized at higher flow conditions (1.5 l min^{-1}) in order to precipitate under optimal flow of about 150 ml min^{-1} passing each discharge (Table 3). The produced aerosol is split in the highly-symmetric tenfold flow splitter and deposited via external EP onto the set of ten secondary platforms (Fig. 3c).

The ETV sampling for CFS is carried out only with internal EP of the aerosol onto the internal platform of the atomizer. I.e. externally precipitated analytes are determined by employing a second ETV-EP process with inserting the ETV-EP loaded “children” platforms again into the ETV. Thus, the “children” samples are subjected to a tandem ETV-EP process. Calibration of the second ETV-EP process is performed against multi-element solutions dosed onto the ETV boat. Besides CFS, several “children” samples were also analyzed with single- and multi-element analytical instruments (SSAAS, ETV-ICP-OES/MS, and ET AAS) in laboratories of Analytik Jena AG and other co-authors of this work after post mailing of the platforms in plastic containers.

3. Results and discussion

3.1. Analytical performance of ETV-FT and ETV-AFC instruments for solid and liquid dosed samples

In our previous works [13-15] TEs provided by the ETV-FT instrument were determined with BCR CRM 189 Wholemeal flour, BCR CRM 281 Rye grass (Institute of Reference Materials and Measurements, Geel, Belgium), NIST SRM 1567 Wheat flour (National Institute of Standards and Technology, Gaithersburg, USA), and with multi-element standard solutions containing approximately the same dosed metal masses as certified for the solid samples. The found concentrations were in good agreement with the certified values and TEs for solid samples were slightly higher than that for liquid samples. This fact was likely caused by incomplete removal of the organic matrix that could act as an additional physical carrier. The measurements showed higher TEs for elements of higher volatility that is in full agreement with Krivan [7] and Kantor [11].

The TE data found with the ETV-FT [15] for the certified reference material BCR 189 Wholemeal flour and for multi-element standard solution containing approximately the same dosed element masses as the solid sample (see Sec. 2.2 for details) were compared with those to be found with the ETV-AFC instrumentation in current study. TEs for ETV-EP sampling were simultaneously determined by calibration of transported analyte masses against the multi-element standard solutions dosed into the HGA furnace of the multi-element CFS spectrometer.

TEs of Mn, Cu, and Fe obtained for both types of the ETV units are shown in Fig. 5. For ETV-FT measurements, 150 ml min^{-1} internal argon flow and no coolant gas flow were used. According to our earlier results [13, 14] the cooling gas had no positive effect on the TE. For ETV-AFC determinations with 1.5 L min^{-1} total gas flow only the tenth fraction of a sample aerosol was dosed into the HGA furnace. The higher total gas flow included 0.2 L min^{-1} of internal gas and 1.3 L min^{-1} of coolant gas (Table 3). As was reported earlier [13, 14], the flow rate through the EP sample capillary higher than 150-200 ml min^{-1} decreases the analyte deposition efficiency. It is evident from Fig. 5 that the TEs obtained with the ETV-AFC instrumentation are 10-20% higher for all sample analytes. This improvement can be explained by preventing analyte condensation at the colder ends of the vaporizer. The somewhat higher analyte TEs observed for solid standards of organic nature is likely caused by incomplete removal of the organic matrix as mentioned above with respect to earlier results.

Although the ETV-AFC instrumentation provides higher TEs, approximately two-thirds of the sample analytes still could not reach the HGA furnace of the CFS spectrometer at this state of the development. The losses obviously occurred due to the low efficiency of sample transformation into aerosol particulates in the AFC zone. I.e. the ETV-AFC unit needs to be further optimized.

3.2. Optimization of the ETV-AFC instrumentation

In current work, the ETV-AFC unit is optimized in following directions. The efficiency of analyte transformation into an aerosol is strongly affected by flow structure within the AFC zone that is under given flow rates governed by the convection tube dimensions. Due to the high buoyant force exert by the surrounding coolant gas flow

(Archimedes' principle) at the ETV-AFC interface, the hot outlet upstream becomes very fast and, if the convection tube is too wide, the upstream drives a counter flowing downstream at the tube walls. The formed whirls and turbulences bring the analyte to the tube walls where their adsorption may occur and reduce the volume density of condensing analyte particulates that in total decrease the efficiency of vapor-aerosol transformation. On the other hand, the AFC should not be too narrow because of analyte losses by its adsorption/condensation on the tube walls. Series of measurements of TEs and studies with smoking samples have been performed and it was found that the optimal size of the AFC tube is about 13 mm inner diameter and 15 cm in length.

Temperature gradients right above the outlet of the graphite tube should be as high as possible in order to facilitate vapor-aerosol transformation. It was found that emission of incandescent ETV walls is a major cause for increased temperatures of the condensing particulates. This negative effect was decreased by shielding the condensation zone against the radiation from the ETV and by surrounding the hot upstream with cooling argon a few millimeters above the outlet hole of the graphite furnace.

3.3. Effect of sample/carrier modifiers on analyte transport efficiency

The results obtained with the modified ETV-AFC instrument are shown in Fig. 6 along with the previous experimental data that were obtained without radiation shielding. TEs of Pb as an element of higher volatility and Cu, Fe, and Ni as elements of medium volatility are determined with the ETV without and with the radiation shielding. Measurements with tenfold aerosol dilution as well as with undiluted samples are carried out. For determination of higher analyte amounts, aerosol dilution with higher bypass flow and 1:9 flow splitting is used. TEs for undiluted samples obtained with the ETV without

shielding are not significantly higher than that obtained with the ETV-FT [15] and not presented in current study. Owing to the increase in TEs, dosed analyte masses and total dosed sample masses for the ETV-EP measurements are reduced approximately by factors of 3-4 and 9, respectively, in comparison with the preceding data.

Some interesting observations can be drawn from Fig. 6. First, the figure shows a marked increase in TEs of all sample analytes with the improved ETV furnace. The differences in TEs for dosing with and without tenfold splitting are also reduced. The higher values found with splitting can likely be attributed to the higher flow rates of internal and coolant gases. 48-50% TEs are obtained with radiation shielding, higher flow conditions (1.5 l min^{-1}), and 1:9 aerosol flow splitting for four simultaneously determined metals - Cu, Fe, Mn, and Pb. The slightly lower TE of the less volatile Ni (44.5%) in this case is likely due to the fact that the vaporization temperature was not high enough to achieve co-vaporization. High and low volatile elements in the improved ETV setup are transported with more equal efficiencies. Furthermore, Fig. 6 shows a significant increase in TE of Cu, Fe, and Ni with the use of potassium, especially at higher flow rates. Dependence of the TE on sample analytes was observed before with both types of the ETV unit, however, in this study the use of the modified vaporizer and optimized flow conditions yields nearly equal TEs for different sample analytes.

Owing to the ETV modification longitudinal temperature gradients in the AFC zone are greatly enhanced. At higher flow conditions and with higher masses, TEs of all sample analytes are increased up to 50%. Less dependence on individual sample analytes is observed.

3.4. Precision and reproducibility of measurements

Reproducible sample transfer from a primary to a secondary platform or to a set of platforms allows micro-dosing of solids or liquids with diluting and dividing of a sample in the aerosol phase. The precision of measurements is within the range of 2-4% RSD (n=4-5) for both diluted and undiluted sample aerosols (see Fig. 6).

TE mean values for Cu, Fe, Mg, Ni, and Pb from the ETV boat to 10 secondary platforms of the external tenfold precipitator are given in Fig. 7. Standard aqueous solution containing twentyfold analyte masses (see Table 2b for details) is employed as a primary sample. Determined TEs are between 42-57% with relative standard deviation 8-12% (n=10). It should be pointed out that analyte compositions on "children" platforms loaded via ETV with external EP are measured with second ETV-EP process, this time with internal precipitation. Therefore, all sample analytes have passed the ETV-EP process twice owing to the tandem procedure. Analysis of "children" samples was also carried out after post mailing in plastic containers in co-authors laboratories with ICP-MS (authors c) and ET AAS (authors b and d) as well as with SSAAS (Analytik Jena AG). This indicates the high stability of the platform adsorbed samples.

Distribution of TEs for Fe and Mn from the primary boat to 10 "children" platforms of the external tenfold precipitator along with mean values is presented in Fig. 8. There is a high correlation in deposited analyte quantities between the platforms of the external precipitator. However, the variation of the TEs and the corresponding deposited masses is not the result of the scatter of aerosol flow rates or corona discharge currents through each precipitator. This variation is most likely caused by a not perfectly reproducible positioning of the graphite platform in the precipitator at the present state of development. This may be a reason that not all discharges burn optimally during the EP process. Blank measurements

under variety of precipitating conditions show the absence of contamination at the precipitator.

4. Conclusions and further perspectives

The novel platform-to-platform sample transfer, distribution, dilution, and dosing system described in this paper allows external sample pretreatment, sampling, and handling with aerosol dosing of a primary solid organic or inorganic, bulk, powder or liquid sample. The ETV instrument described here together with several versions of aerosol flow splitters provides up to three-four times higher transport efficiency as compared to the end-on flow-through ETV developed earlier. Proposed system offers higher transport efficiencies for all analytes studied that are, in addition, more uniform for elements of different volatility. A main feature of the new ETV version is an upstream inside a vertically oriented glass tube creating an axially focusing convection zone, where vapor condensation and aerosol formation take place predominantly apart from the colder walls.

A sample dividing system allows splitting of the sample aerosol and re-collection by electrostatic precipitation of the analytes with equal shares on ten platforms. It provides sample vessels of equal analyte compositions that are suited for control and supplementary measurements with SSAAS, ET AAS, and ICP-MS/OES. Effect of potassium as nitrate (prepared from a standard stock solution) on analyte transport efficiency is shown. As a sample/carrier modifier, potassium promotes analyte condensation and enhances analyte transport efficiency.

This technique rather requires significantly more basic research with the aim to understand the mechanisms involved in the analyte transport process. Main analyte losses in the ETV configuration and the upper limit of the transport efficiency; influences of sample/carrier modifiers on vaporization, aerosol formation, and transport, including effects of high/low volatile analytes in low/high volatile matrices; influence of externally generated carriers (as well as graphite furnace carbon co-vaporized with the analytes) on transport efficiency are the matter of further investigations.

Acknowledgments

The authors are indebted to "International Association for the Promotion of Cooperation with Scientists from the New Independent States of the Former Soviet Union (INTAS)" for financial support and to Schunk Kohlenstoffwerke GmbH, Heuchelheim, Germany for support with graphite parts, to Analytik Jena AG for comparative measurements.

References

[1] U. Kurfürst, Solid sample analysis: direct and slurry sampling using GF-AAS and ETV-ICP, Springer-Verlag, Berlin, Germany, 1998.

[2] T. Kántor, Gy. Záray, Graphite furnace for alternative combination with d. c. arc or inductively coupled plasma, Fresenius J. Anal. Chem. 342 (1992) 927-935.

[3] M.M. Lamoureux, D.C. Grégoire, C.L. Chakrabarti, and D.M. Goltz, Modification of a commercial electrothermal vaporizer for sample introduction into an inductively coupled plasma mass spectrometer. 1. Characterization, Anal. Chem. 66 (1994) 3208-3216.

[4] L. Moens, P. Verrept, S. Boonen, F. Vanhaecke and R. Dams, Solid sampling electrothermal vaporization for introduction in inductively coupled plasma mass spectrometry, Spectrochim. Acta Part B 50 (1995) 463-475.

[5] Gy. Záray, T. Kántor, Direct determination of arsenic cadmium, lead, and zinc in soils and sediments by electrothermal vaporization and inductively coupled plasma excitation spectroscopy, Spectrochim. Acta Part B 50 (1995) 489-500.

[6] C.M. Sparks, J.A. Holcombe, T.L. Pinkston, Sample retention in the transport tubing between an electrothermal vaporizer and inductively coupled plasma mass spectrometer, Appl. Spectrosc. 50 (1996) 86-90.

[7] U. Schäffer, V. Krivan, A graphite furnace electrothermal vaporization system for inductively coupled plasma atomic emission spectrometry, Anal. Chem. 70 (1998) 482-490.

[8] D.C. Grégoire, R.E. Sturgeon, Analyte transport efficiency with electrothermal vaporization inductively coupled plasma mass spectrometry, Spectrochim. Acta Part B 54 (1999) 773-786.

[9] T. Kántor, S.Güçer, Efficiency of sample introduction into inductively coupled plasma by graphite furnace electrothermal vaporization, Spectrochim. Acta Part B 54 (1999) 763-772.

[10] J. Hassler, A. Detcheva, O. Förster, P. Perzl, K. Flórian, Working with a modern ETV-device and an ICP-CID spectrometer, Annali di Chimica, 89 (1999) 827-836.

[11] T. Kantor, Sample introduction with graphite furnace electrothermal vaporization into an inductively coupled plasma: effects of streaming conditions and gaseous phase additives, Spectrochim. Acta, Part B 55 (2000) 431-448.

[12] G. Torsi, F. Palmisano, Particle collection mechanism and efficiency in electrostatic accumulation furnace for electrothermal atomic spectrometry, Spectrochim. Acta Part B 41 (1986) 257-264.

[13] T. Buchkamp, G. Hermann, Solid sampling by electrothermal vaporization in combination with electrostatic particle deposition for electrothermal atomization multi-element analysis, Spectrochim. Acta Part B 54 (1999) 657-668.

[14] J. Bernhardt, T. Buchkamp, G. Hermann, G. Lasnitschka, Transport efficiencies and analytical determinations with electrothermal vaporization employing electrostatic precipitation and electrothermal atomic spectrometry, Spectrochim. Acta Part B 54 (1999) 1821-1829.

[15] J. Bernhardt, T. Buchkamp, G. Hermann, G. Lasnitschka, Sample transport efficiency with electrothermal vaporization and electrostatic deposition technique in multi-element solid sample analysis of plant and cereal materials, Spectrochim. Acta Part B 55 (2000) 449-460.

[16] J. Sneddon, Electrostatic precipitation atomic absorbtion spectrometry, Appl. Spectrosc. V44 (1990) 1562-1565.

[17] T. Buchkamp, A. Garbrecht, G. Hermann, B. Kling, Size and distribution of particles deposited electrostatically onto the platform of a graphite furnace obtained using laser ablation sampling, Spectrochim. Acta Part B 52 (1997) 1525-1533.

[18] R. Torge, Project report Fa, Carl Zeiss Oberkochen, 1980; personal communicationm 1997.

[19] R.W. Fonseca, N.J. Miller-Ihli, C. Sparks, J.A. Holcombe, B. Shaver, Effect of oxygen ashing on analyte transport efficiency using ETV-ICP-MS, Appl. Spectrosc. 51 (1997) 1800-1806.

[20] R.D. Ediger, S.A. Beres, The role of chemical modifiers in analyte transport loss interferences with electrothermal vaporization ICP-mass spectrometry, Spectrochim. Acta Part B 47 (1992) 907-922.

[21] D.M. Hughes, C.L. Chakrabarti, D.M. Goltz, D.C. Grégoire, R.E. Sturgeon, J.P. Byrne, Seawateras multi-component physical carrier for ETV-ICP-MS, Spectrochim. Acta Part B 50 (1995) 425-440.

[22] J.D. Venable, J.A. Holcombe, Signal enhancements produced from externally generated ‘carrier’ particles in electrothermal vaporization-inductively coupled plasma mass spectrometry, Spectrochim. Acta Part B 55 (2000) 753-766.

[23] T. Kántor, Interpreting some analytical characteristics of thermal dispersion methods used for sample introduction in atomic spectrometry, Spectrochim. Acta Part B 43 (1988) 1299-1320.

[24] M. Ito, Continuum spectrum source excited coherent forward scattering spectrometry for detection of elements, Anal. Chem. 52 (1980) 1592-1595.

[25] L.A. Davis, J.D. Winefordner, Evaluation of a Voigt effect coherent forward scattering atomic spectrometer, Anal. Chem. 59 (1987) 309-312.

[26] G. Hermann, Coherent forward scattering spectroscopy (CFS): present status and future perspectives, Crit. Rev. Anal. Chem. 19 (1988) 323-377.

[27] G. Hermann, Coherent forward scattering atomic spectrometry, Anal. Chem., 64 (1992) 571A-579A.

Tables list

Tables

Table 1
(a) ETV operating conditions

Step	Temperature (°C)	Ramp time (s)	Hold time (s)	Flow conditions (ml min^{-1})
Dry	120	30	10	1500 (flow through)
Pyrolysis	350	30	30	1500 (flow through)
Cool down	20	1	20	150/1500 (upstream)[a]
Vaporize	2600	0	8	150/1500 (upstream)
Cool down	20	1	30	150/1500 (upstream)
Clean	2650	0	6	1500 (flow through)

[a] Details for flow distribution with/without 1:9 splitting see in Table 3

(b) HGA-600 operating conditions

Step	Temperature (°C)	Ramp time (s)	Hold time (s)	Internal gas flow rate (ml min^{-1})
Dry	90	15	15	300
Dry	120	10	20	300
Pyrolysis	400	10	10	300
Cool down	20	1	9	300
Atomize	2500	0	6	0
Cool down	20	1	9	300
Clean	2600	0	6	300

Table 2

(a) Element concentration in the BCR CRM 189 Wholemeal flour and in the respective multi-element standard aqueous solution

Element	Certified concentration[a] BCR CRM 189 (mg kg^{-1})	Concentration[b] Aqueous stock solution (mg l^{-1})
Ca	(520)	13
Cd	0.0713 ± 0.0030	1.75×10^{-3}
Cu	6.4 ± 0.2	0.16
Fe	68.3 ± 1.9	1.71
K	(6300)	157.5
Na	(40)	1
Mg	(1900)	47.5
Mn	63.3 ± 1.6	1.58
Ni	(0.38)	9.5×10^{-3}
Pb	0.379 ± 0.012	9.5×10^{-3}
Zn	56.5 ± 1.7	1.4

[a]Values in brackets are not certified.
[b]After adequate pre-dilution (20 µl dosing)

(b) Element concentration in the multi-element standard solution for measurements with an added modifier

Element	Wavelength of evaluated line (nm)	Concentration[c] (mg l^{-1})	Concentration[d] (mg l^{-1})
Mn	279.8	0.02	0.2
Pb	283.3	0.1	1
Ni	300.2, 305.1	0.5	5
Fe	302.1	0.1	1
Al	308.2	0.1	1
Cu	324.8	0.1	1

[c]Used for the measurements without flow splitting (20 µl dosing)
[d]Used for the measurements with 1:9 flow splitting (20 µl dosing) and with the external tenfold precipitator (40 µl dosing)

Table 3
Flow conditions for the ETV system

Step	Transport without flow splitting		Transport with 1:9 splitting or with external tenfold precipitator	
	Internal gas ($ml\ min^{-1}$)	Coolant gas ($ml\ min^{-1}$)	Internal gas ($ml\ min^{-1}$)	Coolant gas ($ml\ min^{-1}$)
Dry	1000	500 (flow through)	1000	500 (flow through)
Pyrolysis	1000	500 (flow through)	1000	500 (flow through)
Cool down	70	80 (upstream)	200	1300 (upstream)
Vaporize	70	80 (upstream)	200	1300 (upstream)
Cool down	70	80 (upstream)	200	1300 (upstream)
Clean	1000	500 (flow through)	1000	500 (flow through)

Figure captions

Fig. 1. Schematic diagram of the experimental arrangement with electrothermal vaporization and internal electrostatic precipitation for coherent forward scattering spectrometry.

Fig. 2. (a) Schematic representation of the electrothermal vaporization furnace with an axially focusing convection zone (ETV-AFC). The right side window is open during loading, drying, and pyrolysis steps. (b) Photograph of the laboratory constructed ETV-AFC furnace. A pair of tweezers for reproducible transfer of sample vessels shown in the right part.

Fig. 3. Principle of aerosol transport, splitting, and dilution: (a) aerosol transport with internal or external deposition, (b) aerosol transport and dilution, and (c) aerosol transport and splitting.

Fig. 4. Photographs of the laboratory constructed aerosol dividing system and precipitator: (a) external tenfold precipitator, (b) symmetric aerosol flow splitter,
(c) precipitator, (d) the precipitator in the opened state, (e) boats with adapters.

Fig. 5. Transport efficiencies of Cu, Fe and Mn obtained with BCR CRM 189 Wholemeal flour and with aqueous solutions according to Table 2a; standard deviations for n=4-5.
End-on flow-through ETV (ETV-FT): ▨ 30 µg CRM for Mn, 500 µg for Cu and Fe;
□ dosed multi-element solution containing the same analyte masses as the solid sample.
ETV with axially focusing convection zone (ETV-AFC), 1:9 flow splitting:
▨ 250 µg CRM for all measurements; □ dosed multi-element solution containing the same analyte masses as the solid sample.

Fig. 6. Transport efficiencies of Cu, Fe, Ni, and Pb dosed as liquid solution into the graphite boat of the ETV; standard deviations for n=4-5. Measurements without and with 1 µg K or Pd as a sample/carrier modifier.

☐ ETV-AFC without radiation shielding of the condensation zone, transport with 1:9 splitting and with 1.5 l min^{-1} total flow, analyte masses: 64 ng Cu, 64 ng Fe, 640 ng Ni, and 64 ng Pb.

▨ ETV-AFC with radiation shielding of the condensation zone, transport without splitting and with 150 ml min^{-1} total flow, analyte masses according to Table 2b.

☒ ETV-AFC with radiation shielding of the condensation zone, transport with 1:9 splitting and with 1.5 l min^{-1} total flow, analyte masses according to Table 2b.

Fig. 7. Boat-to-platform transport efficiencies of Cu, Fe, Mn, Ni, and Pb dosed as liquid solution into the ETV boat obtained with tenfold aerosol splitter and external tenfold precipitator (n=10, i.e. over all EP stations and with full tandem ETV-EP procedure). Analyte masses according to Table 2b.

Fig. 8. Distribution and mean value of transport efficiencies for Fe (▨) and Mn (☐) from the primary boat to 10 secondary platforms of the external tenfold precipitator dosed into the ETV boat as liquid solution (tandem ETV-EP procedure). Analyte masses according to Table 2b.

Figures

Fig. 1

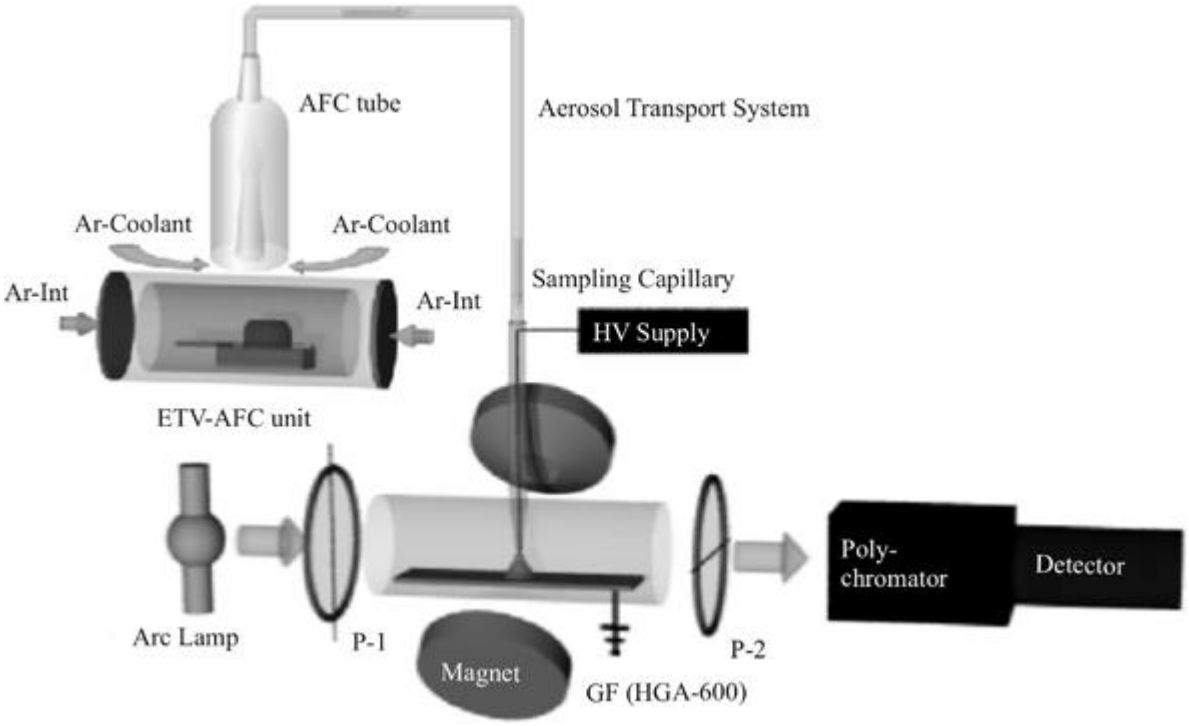

Fig. 2

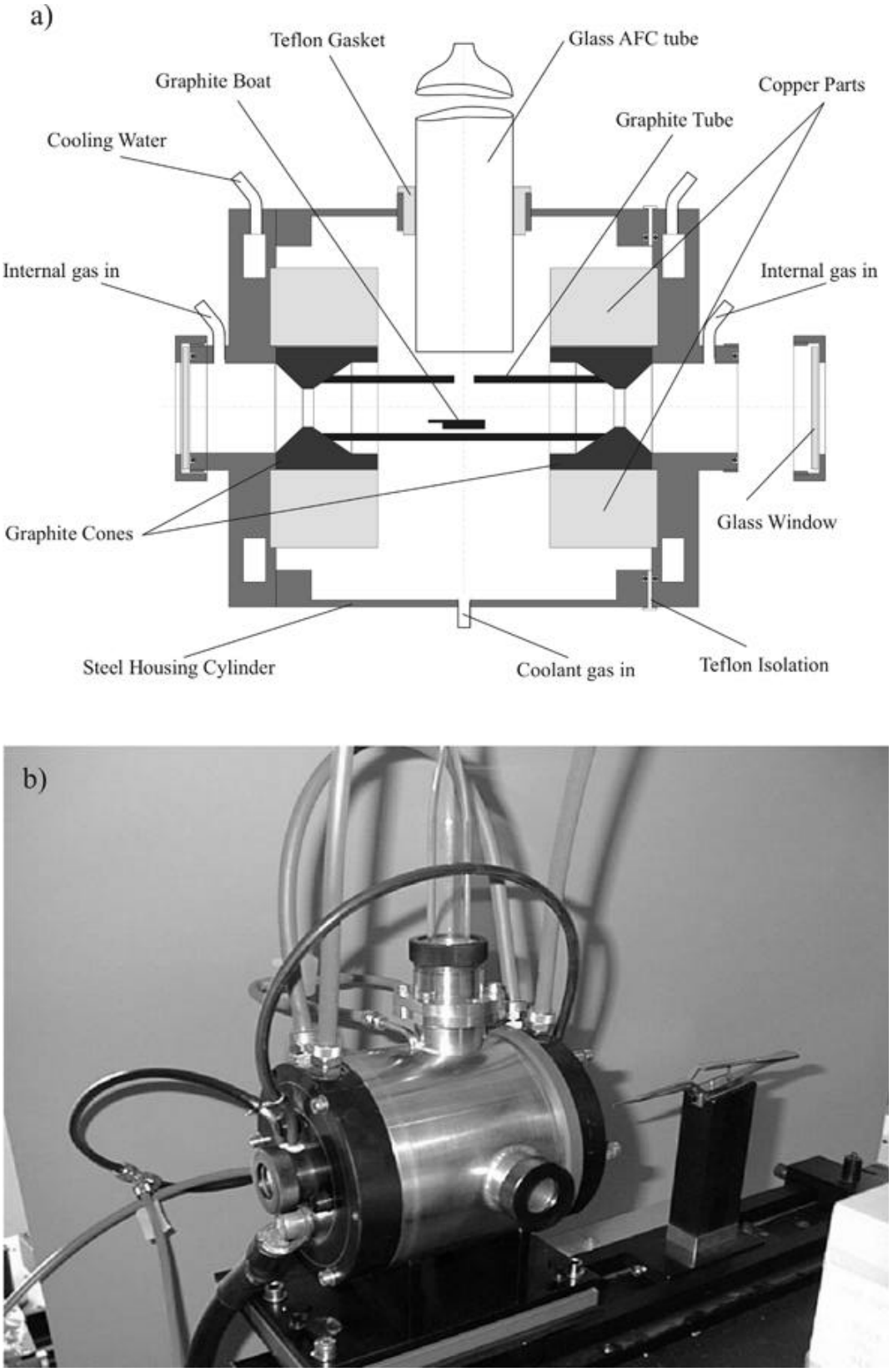
a)
Teflon Gasket
Glass AFC tube
Graphite Boat
Copper Parts
Graphite Tube
Cooling Water
Internal gas in
Internal gas in
Graphite Cones
Glass Window
Steel Housing Cylinder
Coolant gas in
Teflon Isolation
b)

Fig. 3

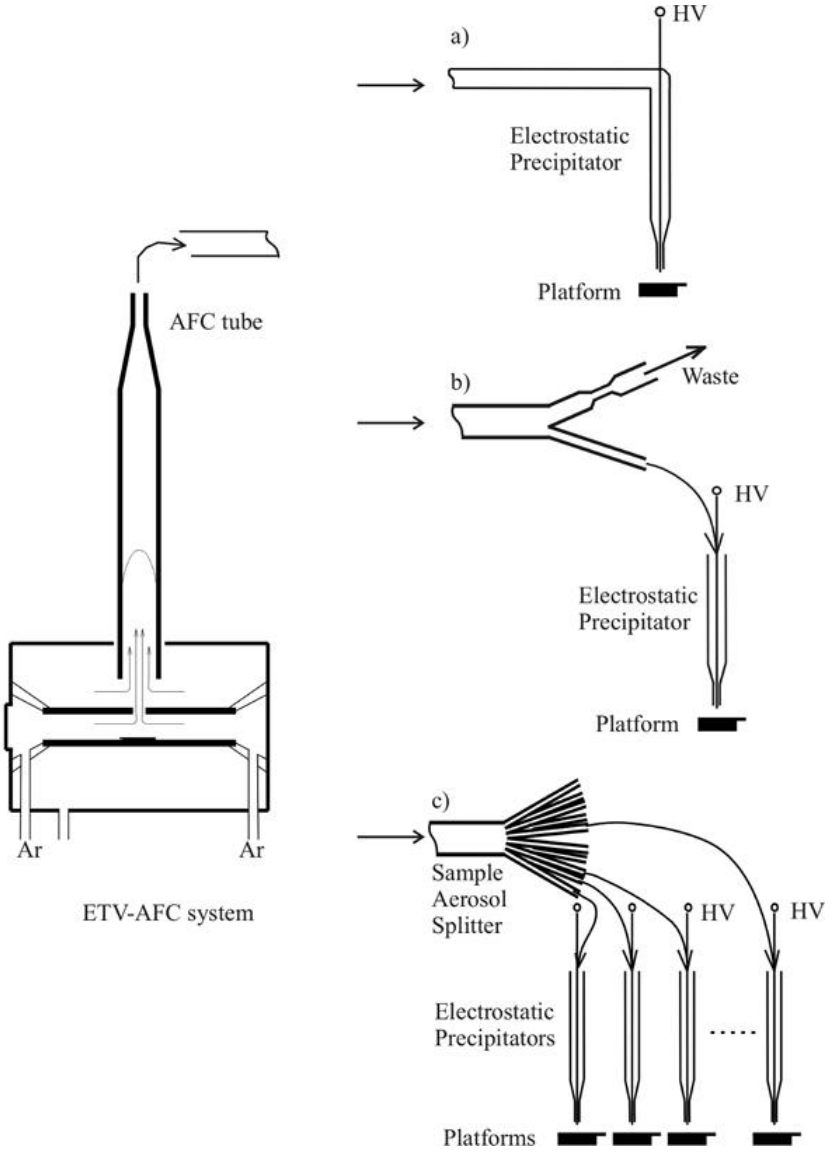
a)
HV
Electrostatic
Precipitator
Platform
b)
Waste
HV
Electrostatic
Precipitator
Platform
c)
Sample
Aerosol
Splitter
HV
HV
Electrostatic
Precipitators
Platforms
AFC tube
Ar
Ar
ETV-AFC system

Fig. 4

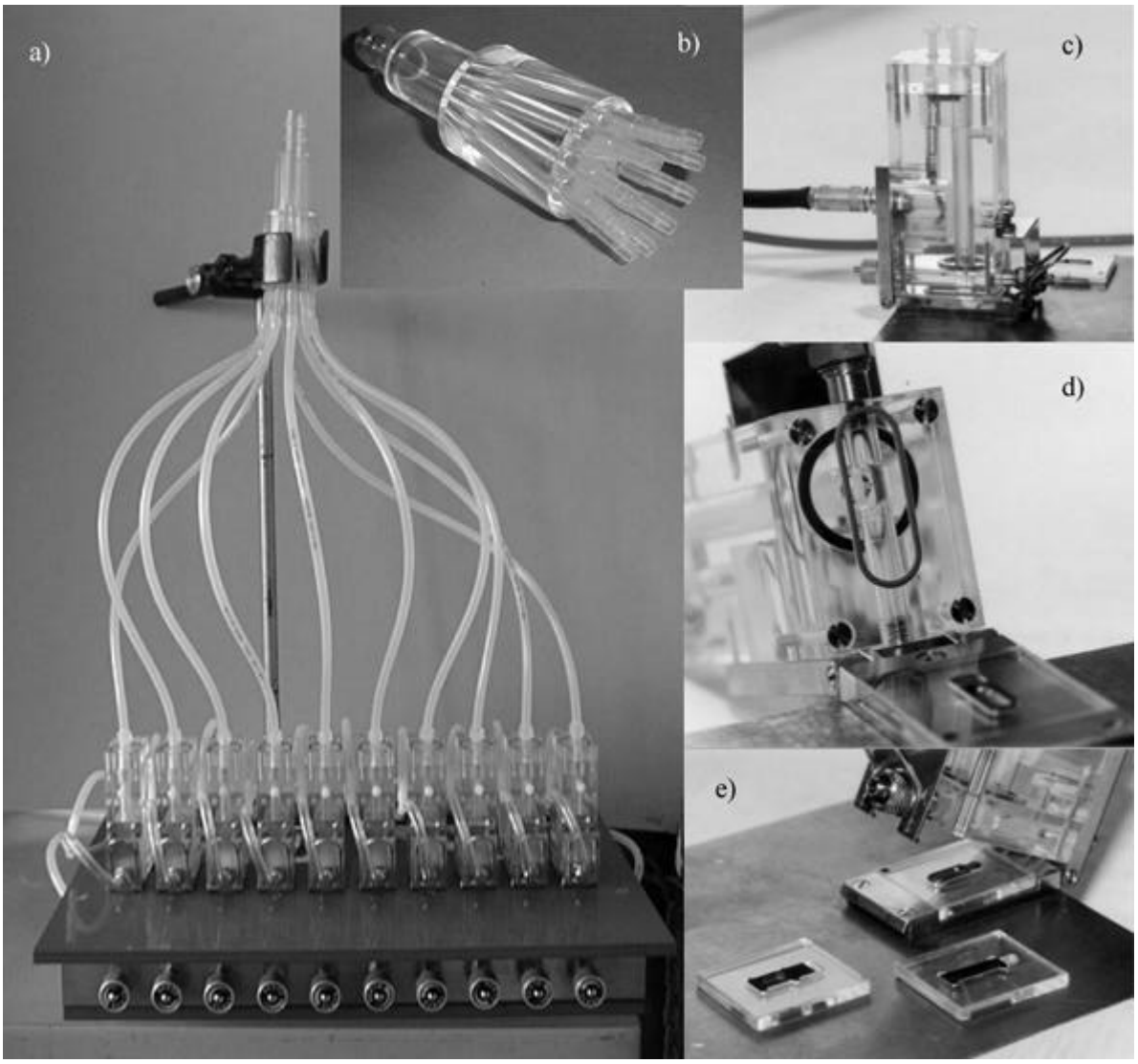

Fig. 5

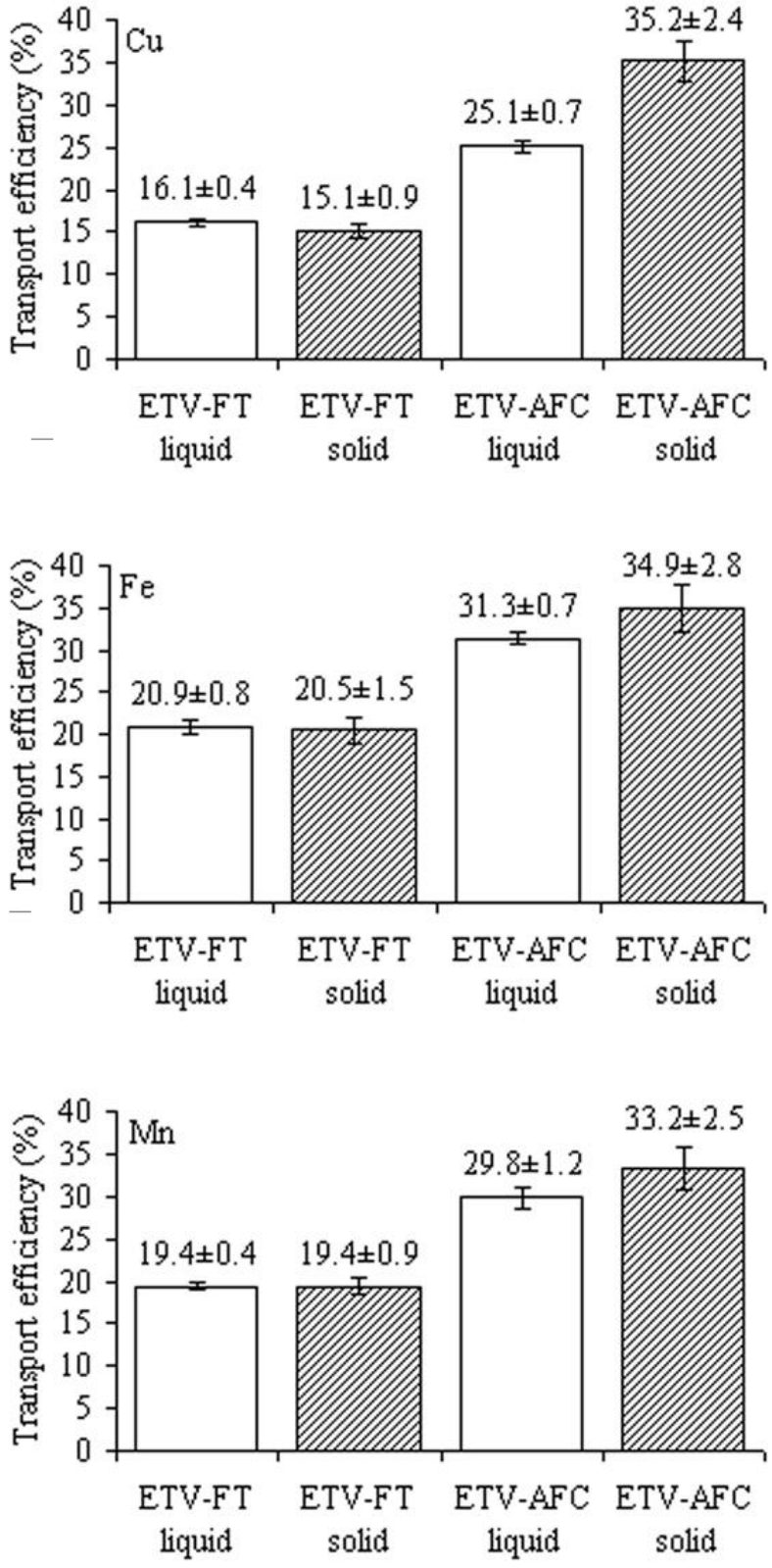
Cu
Transport efficiency (%)
40
35
30
25
20
15
10
5
0
16.1±0.4
15.1±0.9
25.1±0.7
35.2±2.4
ETV-FT liquid
ETV-FT solid
ETV-AFC liquid
ETV-AFC solid
Fe
Transport efficiency (%)
20.9±0.8
20.5±1.5
31.3±0.7
34.9±2.8
ETV-FT liquid
ETV-FT solid
ETV-AFC liquid
ETV-AFC solid
Mn
Transport efficiency (%)
19.4±0.4
19.4±0.9
29.8±1.2
33.2±2.5
ETV-FT liquid
ETV-FT solid
ETV-AFC liquid
ETV-AFC solid

Fig. 6

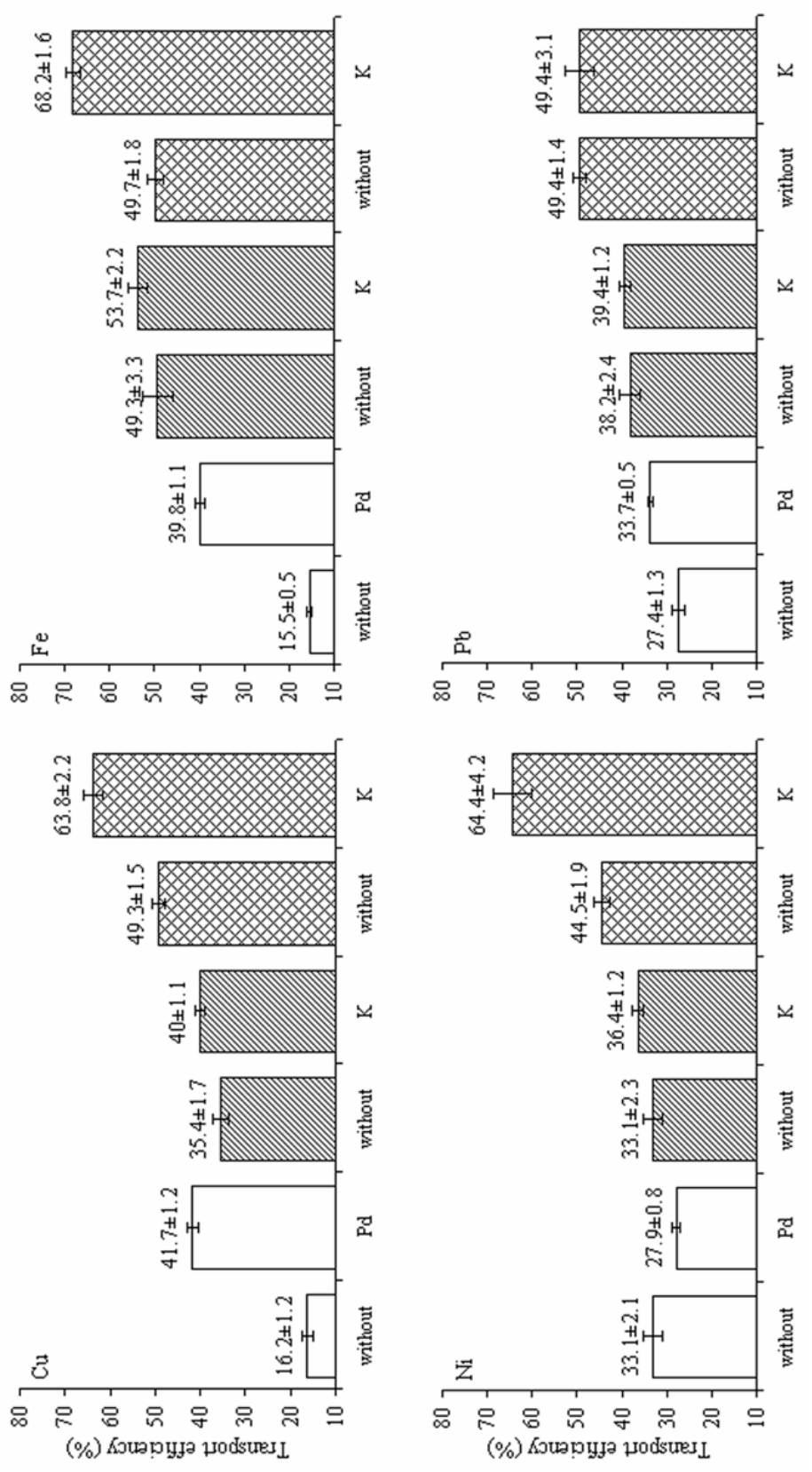
Cu
Fe
Ni
Pb
Transport efficiency (%)
without
Pd
without
K
16.2±1.2
41.7±1.2
35.4±1.7
40±1.1
49.3±1.5
63.8±2.2
15.5±0.5
39.8±1.1
49.3±3.3
53.7±2.2
49.7±1.8
68.2±1.6
33.1±2.1
27.9±0.8
33.1±2.3
36.4±1.2
44.5±1.9
64.4±4.2
27.4±1.3
33.7±0.5
38.2±2.4
39.4±1.2
49.4±1.4
49.4±3.1

Fig. 7

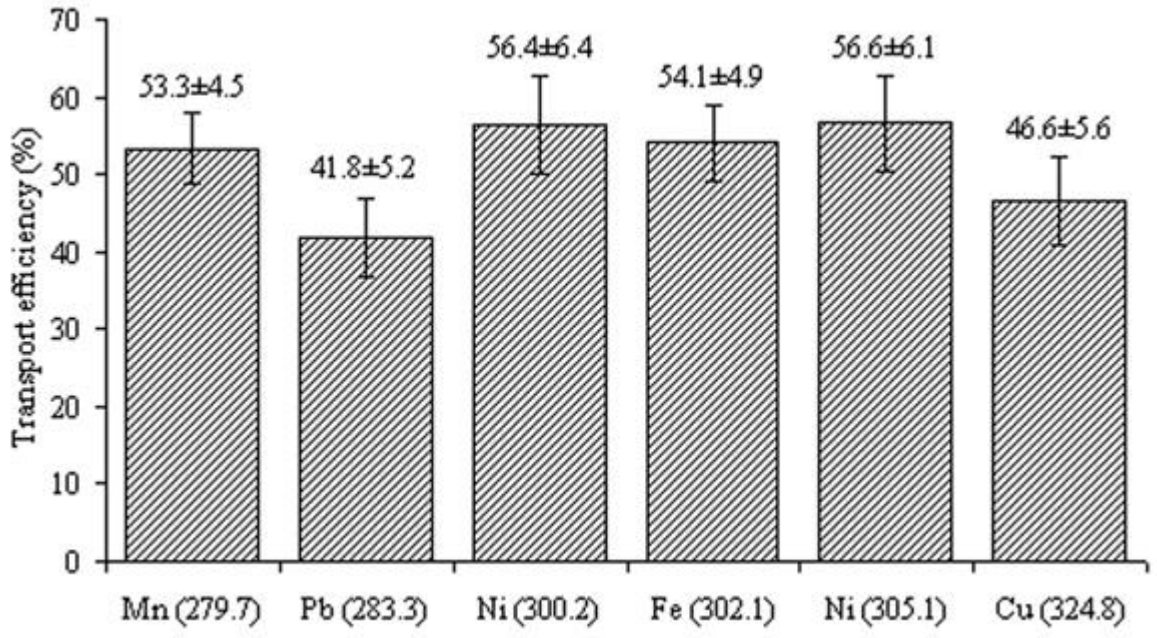
Transport efficiency (%)
70
60
50
40
30
20
10
0
53.3±4.5
41.8±5.2
56.4±6.4
54.1±4.9
56.6±6.1
46.6±5.6
Mn (279.7)
Pb (283.3)
Ni (300.2)
Fe (302.1)
Ni (305.1)
Cu (324.8)

Fig. 8

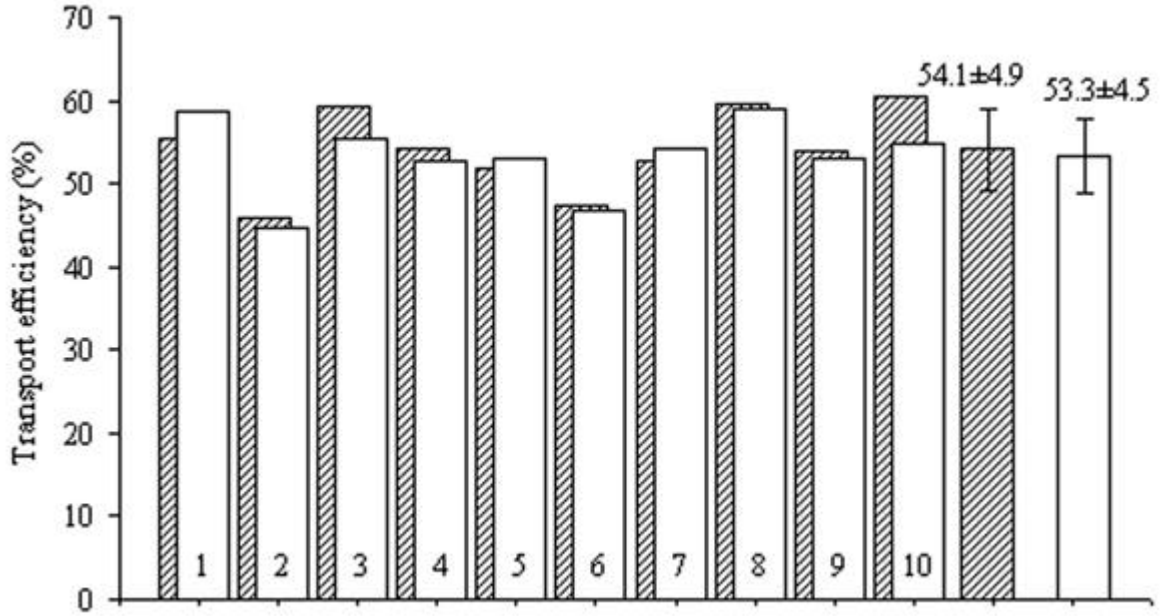
Transport efficiency (%)
70
60
50
40
30
20
10
0
1
2
3
4
5
6
7
8
9
10
54.1±4.9
53.3±4.5